

Performance Analysis of Matrix Converter Fed Induction Motor with Different Switching Algorithms

C. Ponmani^{1*} and M. Rajaram²

¹**Department of Electrical Engineering,
Government College of Engineering, Tirunelveli, India*
²*Anna University of Technology, Tirunelveli, India*
**Corresponding Author E-mail: josy_cp@yahoo.com*

Abstract

Switching algorithms of Matrix converter such as Venturini control algorithm, Space vector modulation (SVM) and carrier based modulation methods are simulated here. The values of third, fifth and seventh harmonics of output voltage fed to the induction motor in terms of percentage of fundamental output voltage is measured for all the three methods and compared with each other. The output voltage transfer ratio of all the switching algorithms is also verified by using Fourier analysis block in Simulink. Finally the dynamic performance of the induction motor fed with matrix converter is analyzed for different switching algorithms. The proposed system is validated using Matlab/Simulink simulation and analysis.

Keywords: Dynamic performance, Harmonic analysis, Induction Motor, Matrix Converter, Switching algorithms, Voltage Transfer Ratio.

Introduction

Matrix converter has diverse applications and it does not need any dc-link circuit and large energy storage elements. Different modulation methods for matrix converter are proposed by researchers. Venturini algorithm and enhanced modified venturini algorithm are proposed by Alesina and Venturini [1]. Huber et al [7] proposed the principles of Space Vector Modulation applied to the Matrix Converter. Yoon and Sul [9] presented carrier-based modulation technique for matrix converter. Comparison of modulation methods is very much essential to use it any application. Apap et al [2] presented a comparison between venturini and SVM methods in terms of device power loss and distortion at the input current and output voltage. Zhou et al [11] presented a relationship between space vector modulation and carrier based

modulation such as the relationship between modulation signals, space vectors, the space-vector sectors and the switching pattern. Ghalem Bachir et al [5] presented a comparison between scalar and venturini modulation methods with different frequencies of operation. Comparison of modulation methods in terms of output voltage is very much essential to analyze the power quality of output power as well as the input power. In this paper, comparison of modulation methods with different frequencies of operation and the odd harmonics presented in terms of percentage of fundamental components of output voltage are measured and compared with each other. In addition to that induction motor speed torque response and dynamic performance is also analyzed with all the switching algorithms.

Theory of Matrix Converter

The basic diagram of a matrix converter can be represented by Figure 1. The symbol S_{ij} represents the ideal bidirectional switches, where i represent the index of the output voltage and j represents the index of the input voltage. Let $[V_i]$ be the vector of the input voltages given as:

$$[V_i] = V_{im} \begin{bmatrix} \cos \omega_i t \\ \cos(\omega_i t - 2\pi/3) \\ \cos(\omega_i t - 4\pi/3) \end{bmatrix} \tag{1}$$

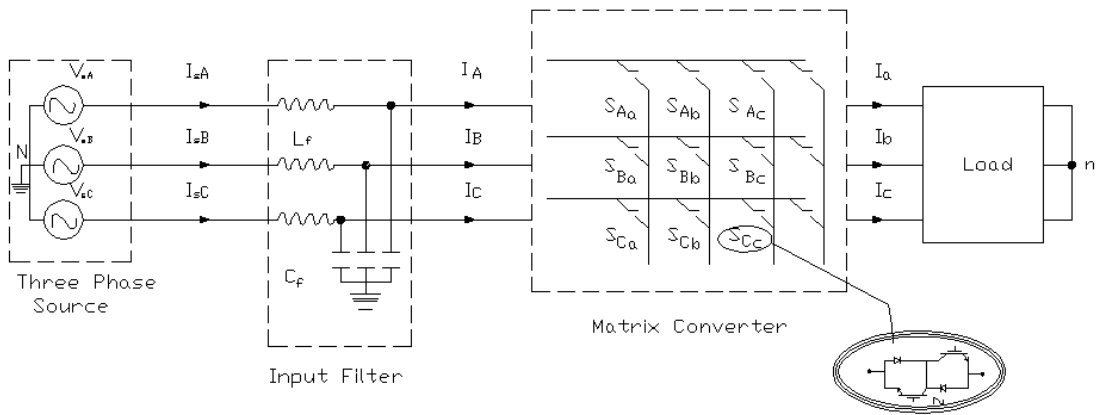


Figure 1: Basic diagram of a matrix converter.

$[V_o]$ is the vector of output voltages,

$$[V_o] = V_{om} \begin{bmatrix} \cos \omega_0 t \\ \cos \omega_0 t - 2\pi/3 \\ \cos \omega_0 t - 4\pi/3 \end{bmatrix} \tag{2}$$

The problem consists in finding a matrix M, known as the modulation matrix, such that

$$[V_o]=[M]. [V_i] \tag{3}$$

While, input current [I_i] and output current are related as

$$[I_i]=[M]^T [I_o] \tag{4}$$

where $[M]^T$ represents the transposed matrix of [M]. While, input current [I_i] and output current [I_o] are related during commutation, the bidirectional switches must function according to the following rules [5]. At every instant t, only one switch S_{ij} (i=A,B,C) works in order to avoid short circuit between the phase. At every instant t, at least two switches S_{ij} (j = a, b, c) works to ensure a closed loop load current. The switching frequency $f_s = \frac{\omega_s}{2\pi}$ must have a value twenty times higher than the maximum of f_i, f_o (f_s >> 20. Max (f_i, f_o)). According to Azeddine et al [3], during the period T_s known as sequential period which is equal to 1/f_s, the sum of the time of conduction being used to synthesize the same output phase, must be equal to T_s. Now a time t_{ij} called time of modulation, can be defined as:

$$t_{ij} = m_{ij} \cdot T_s \tag{5}$$

Venturini’s Modulation Method

The new strategy in which the targeted output voltage matrix V_o(t) includes the third harmonics of the input and output frequencies is the Venturini’s Optimum Method. It makes use of the common addition technique. As the target output voltages include third harmonics, the maximum theoretical output to input voltage ratio q, can be increased up to 86%. The voltage transfer ratio is the ratio of output fundamental to input fundamental and its maximum value is 0.866.

$$[v_o(t)] = qV_{im} \begin{bmatrix} \cos(w_0t) - \frac{1}{6} \cos(3w_0t) + \frac{1}{2\sqrt{3}} \cos(3w_0t) \\ \cos\left(w_0t + \frac{2\pi}{3}\right) - \frac{1}{6} \cos(3w_0t) + \frac{1}{2\sqrt{3}} \cos(3w_0t) \\ \cos\left(w_0t + \frac{4\pi}{3}\right) - \frac{1}{6} \cos(3w_0t) + \frac{1}{2\sqrt{3}} \cos(3w_0t) \end{bmatrix} \tag{6}$$

Here the triple harmonics in the input frequency as well as in the output frequency are added. The Modulation Function (m_{Kj}) can be expressed as follows:

$$m_{Kj} = \frac{t_{Kj}}{T_{seq}} = \frac{1}{3} \left(1 + \frac{2v_k V_j}{V_{im}^2} \right) \text{ for } K = A, B, C \text{ and } j = a, b, c \tag{7}$$

where V_{im} is the average input voltage. When unity displacement factor is required

equation (7) becomes:

$$m_{Kj} = \frac{1}{3} \left(1 + \frac{2v_k V_j}{V_{im}^2} + \frac{4q}{3\sqrt{3}} \sin(w_i t + \beta_k) \sin(3w_i t) \right) \quad (8)$$

for $K = A, B, C$ and $j = a, b, c$.

$$\beta_k = 0, \frac{2\pi}{3}, \frac{4\pi}{3}$$

for $K = A, B, C$ respectively. This implementation is readily handled up to switching frequencies of tens of kHz by modern microprocessors. By introducing a phase shift between the actual input voltages and input voltages, V_k input displacement factor control can be introduced in the equation (6). If the displacement factor is different from unity the output voltage limit will be reduced from $0.86V_{im}$ to a lesser value which depends on displacement factor achieved in the input. Therefore the output voltage must be lower than 86% of the input voltage.

Space Vector Modulation

The analysis of Space Vector Modulation method involves the concept of Space Phasor. The Space Phasor method was initially used to represent and analyze three phase machines. This method is particularly used in the area of vector control and also allows the visualization of the spatial and time relationships between the resultant current and flux vectors in various references. For Matrix Converter operation using a space vector approach one and only one switch in each output has to conducting, which leads to twenty seven possible switching combinations. The output voltage vector is:

$$\vec{v}_o(t) = (qV_{im}\sqrt{3})\cos(w_o t) \quad (9)$$

The output voltage vector has a constant length of $qV_{im}\sqrt{3}$ and it is rotating at a frequency w_o . The basis of space vector modulation technique is that the possible output voltages can be expressed in the same form as follows:

$$\vec{v}_o(t) = \frac{2}{3}(v_{10} + av_{20} + a^2v_{30}) \quad (10)$$

Where v_{10}, v_{20}, v_{30} are the output phase voltages and $a \equiv e^{j2\pi/3}$

The corresponding output current vector is given by:

$$\vec{i}_o(t) = \frac{2}{3}(i_{1i} + ai_{2i} + a^2i_{3i}) \quad (11)$$

Where i_{1i}, i_{2i}, i_{3i} are the input line currents. At each sampling instant, the position of the output voltage vector is compared with possible vectors and the desired output is synthesized by time averaging (within the switching interval) between adjacent vectors to give the correct mean voltage. Using a Matrix Converter for this process is

little more complex when compared with using it in a conventional DC link inverter as there are twenty seven possible switching states and input voltages are time varying. In three-phase to three-phase Matrix Converter there are twenty seven possible switching states and the output voltage states may be categorized into three groups.

Group 1: These combinations result when any two output phases are connected to the same input phase. There are eighteen combinations where output voltage and input current vectors have same directions with magnitudes that vary with input voltage phase angle and output current phase angle respectively.

Group 2: When all three output phases are connected to the same input phase we get three combinations giving null output voltage and input current vectors.

Group 3: It includes six combinations in which each output phase is connected to a different input phase. Both magnitude and phase of the resultant vectors are variable in these cases.

Carrier based modulation

In the novel carrier based scheme the need of sector information for calculating duty cycle ratios and so the corresponding look-up tables are avoided. Therefore the output voltage is synthesized to its maximum capacity, $\sqrt{3}/2$ times the amplitude of the input

voltage. This also allows the input power factor to be controlled. The output voltage at each phase is synthesized by time-weighting the three input voltages by the duty ratios. The duty ratios should be chosen that the output voltage remains independent of input frequency. The three-phase balanced input voltages can be considered to be in synchronous reference frame, so that input frequency term will be absent in the output voltage. And so the duty ratios d_{aA} , d_{bB} , d_{cC} are chosen to be $k_A \cos(\omega t - \rho)$, $k_A \cos(\omega t - 2\pi/3 - \rho)$, $k_A \cos(\omega t - 4\pi/3 - \rho)$.

The output voltage at phase A:

$$v_A = k_A \hat{V} \left[\begin{array}{l} \cos(\omega t) \bullet \cos(\omega t - \rho) + \cos(\omega t - 2\pi/3) \bullet \cos(\omega t - 2\pi/3 - \rho) \\ + \cos(\omega t - 4\pi/3) \bullet \cos(\omega t - 4\pi/3 - \rho) \end{array} \right] \quad (12)$$

$$\begin{aligned} v_A &= \frac{3}{2} k_A \hat{V} \cos(\rho) \\ &= \left(\frac{3}{2} k \hat{V} \cos(\rho) \right) \cos(\omega_s t) \end{aligned} \quad (13)$$

This implies that the output voltage depends on $\cos(\rho)$ which in turn depends on input power factor. According to the above expression we could conclude that v_A is independent of the input frequency and only depends on the amplitude \hat{V} of the input voltage where modulation index k_A is a time-varying signal with desired output

frequency ω_o . If the duty ratios are negative then they can't be practically realized. To overcome this drawback offset duty ratios are introduced so that the resultant duty ratios of the individual switches are always positive. That is common-mode voltages in the output are added to the offset duty-ratios. Considering the output phase A:

$$d_{aA} + d_{bB} + d_{cC} = k_A \cos(\omega t - \rho) + k_A \cos(\omega t - 2\pi/3 - \rho) + k_A \cos(\omega t - 4\pi/3 - \rho) = 0 \quad (14)$$

To cancel the negative components from individual duty ratio absolute value of the duty ratios are added. The addition of the common-mode duty-ratio in all switches will maintain the output voltages and input currents unaffected. The input currents are synthesized by time-weighting the output currents by the duty-ratios. The common mode term will produce null current in the input. This can be represented as:

$$(\text{The common mode term}) \times (i_A + i_B + i_C) = 0 \quad (15)$$

The input current of phase A:

$$i_a = (k_A i_A + k_B i_B + k_C i_C) \cos(\omega t - \rho) \quad (16)$$

where k_A , k_B , k_C and i_A , i_B , i_C are three-phase sinusoidal quantities at the output frequency. Also

$$k_A i_A + k_B i_B + k_C i_C = \frac{3}{2} k I_o \cos \phi_o \quad (17)$$

where k is the amplitude of the modulation indices k_A , k_B and k_C and I_o is the amplitude of output currents and ϕ_o is the output power factor angle. From equation 16 we could understand that input current i_a is in a lagging phase of ρ with input voltage v_a . For achieving unity power factor operation ρ has to be chosen equal to zero.

Discussion of Simulation Results

The output voltage waveform in Venturini Method at 40Hz frequency is given in the fig.2 and its corresponding Harmonic Spectrum is shown in the fig.3. Similarly, the output voltage and its corresponding Harmonic Spectrum at a frequency of 50Hz in Venturini Method are given in the fig.4 and fig.5 respectively. Likewise, the output voltage and its Harmonic Spectrum waveform at 60Hz using Venturini Method are given in the fig.6 and fig.7. The output voltage waveform in Space Vector Method at 40Hz frequency is given in the fig.8 and its corresponding Harmonic Spectrum is shown in the fig.9. The output voltage and its corresponding Harmonic Spectrum at a frequency of 50Hz for Space Vector Method are given in the fig.10 and fig.11 respectively. Similarly, the output voltage and its Harmonic Spectrum waveform at 60Hz using Space Vector Method are shown in the fig.12 and fig.13. The values of the various observations are being tabulated in table.1 and are compared.

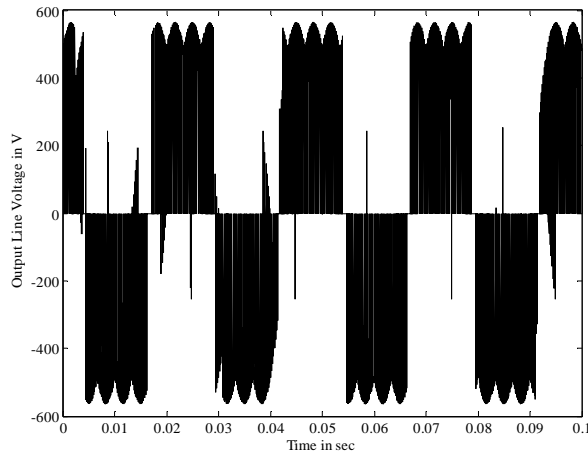


Figure 2: Output voltage in Venturini method for 40Hz.

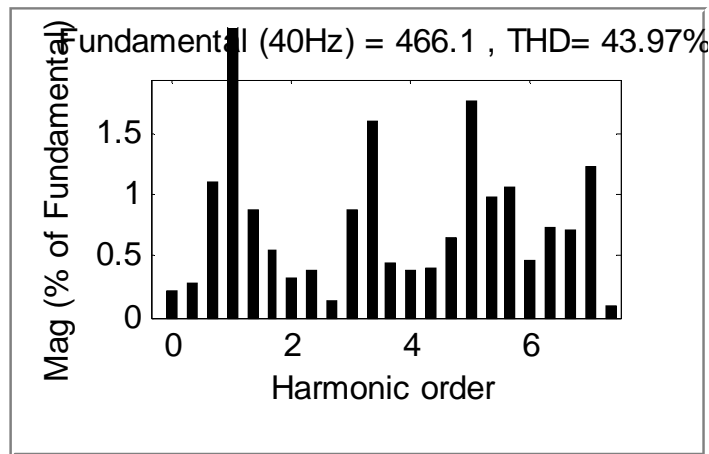


Figure 3: Harmonic Spectrum of output voltage in venturini method for 40Hz.

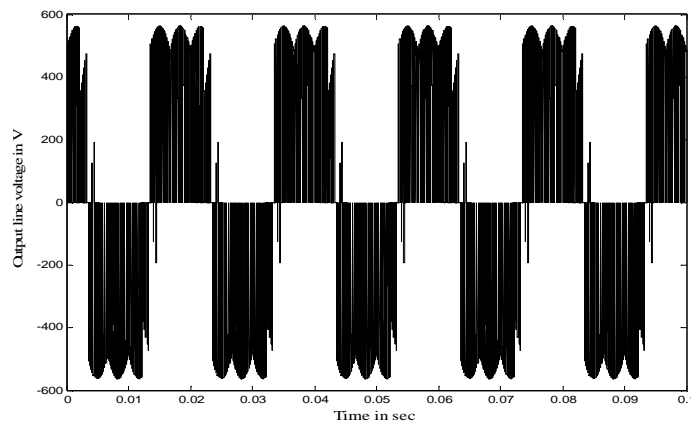


Figure 4: Output voltage in Venturini method for 50Hz.

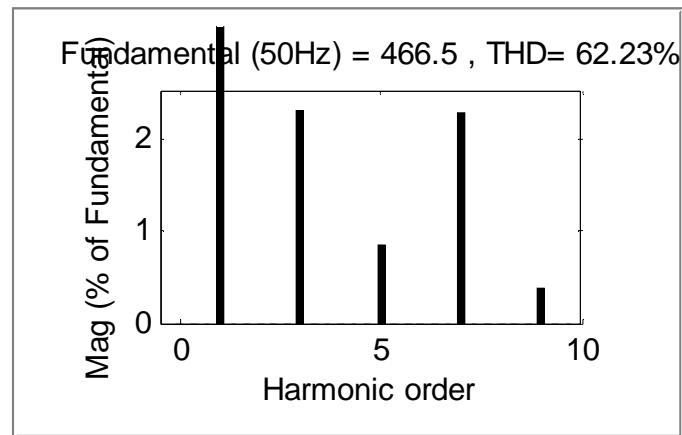


Figure 5: Harmonic Spectrum of output voltage in venturini method for 50Hz.

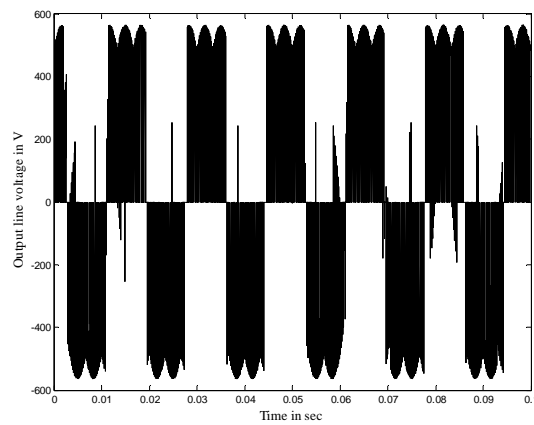


Figure 6: Output voltage in Venturini method for 60Hz.

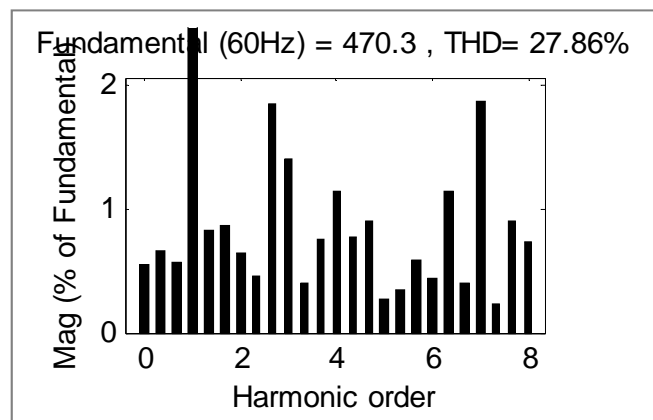


Figure 7: Harmonic Spectrum of output voltage in venturini method for 60Hz.

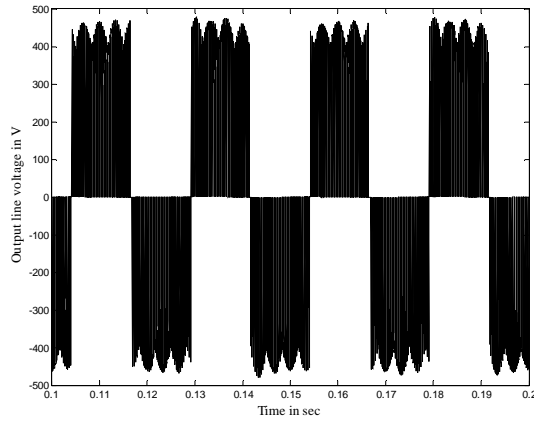


Figure 8: Output voltage in SVM method for 40Hz.

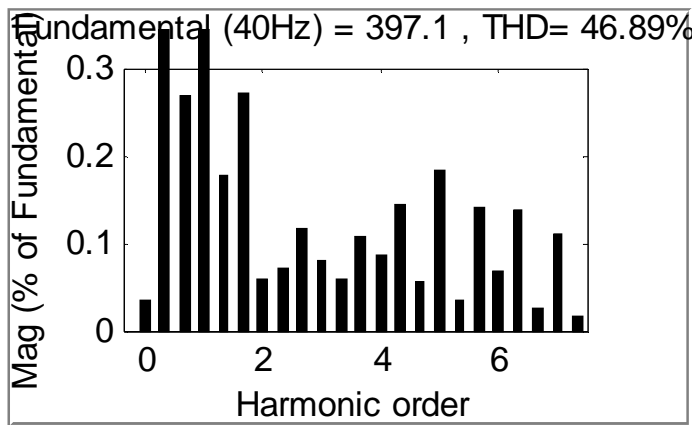


Figure 9: Harmonic Spectrum of output voltage in SVM method for 40Hz.

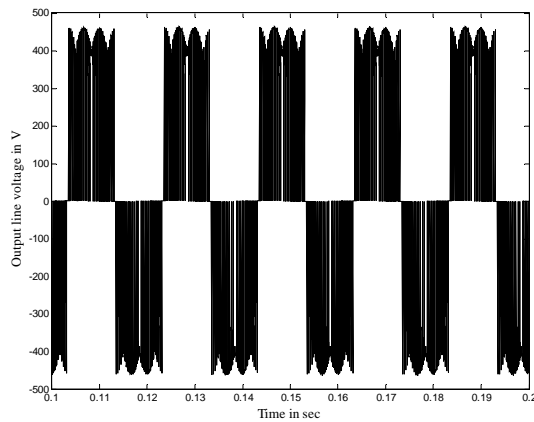


Figure 10: Output voltage in SVM method for 50Hz.

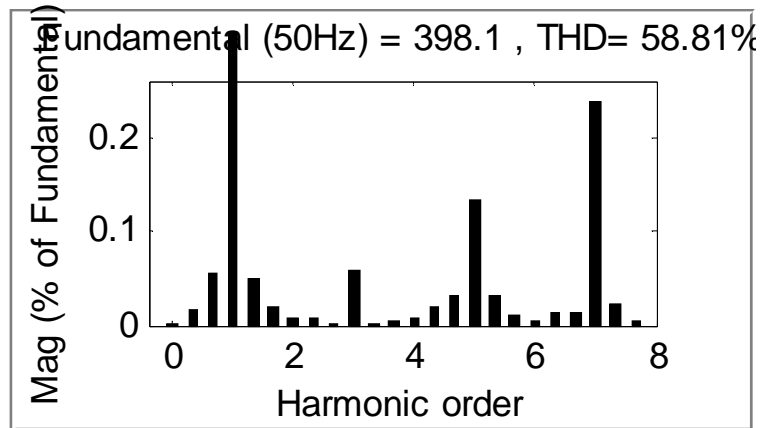


Figure 11: Harmonic Spectrum of output voltage in SVM method for 50Hz.

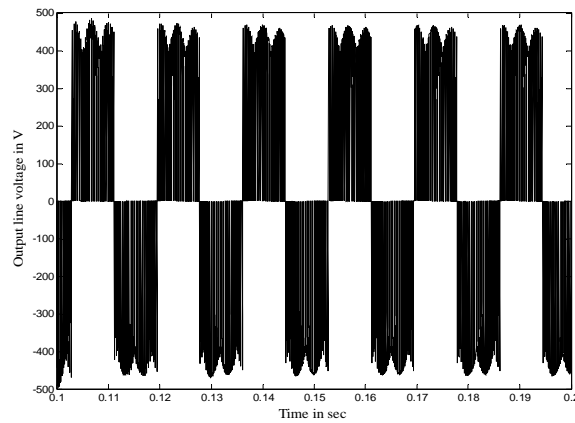


Figure 12: Output voltage in SVM method for 60Hz.

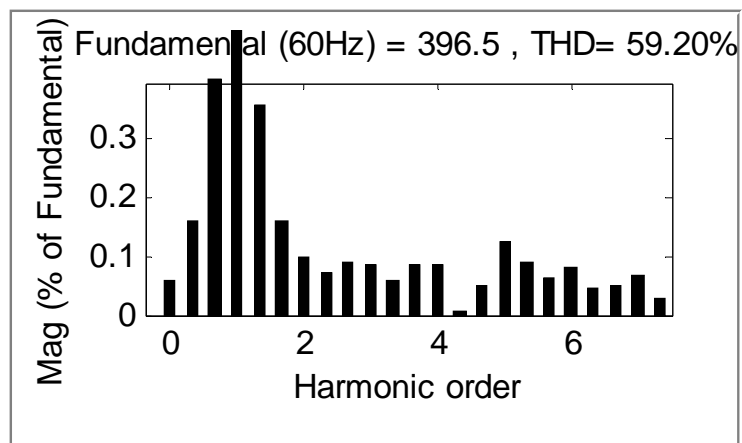


Figure 13: Harmonic Spectrum of output voltage in SVM method for 60Hz.

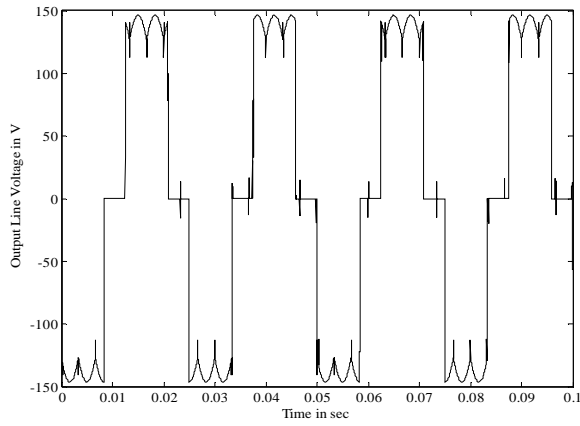


Figure 14: Output voltage in carrier based method for 40Hz.

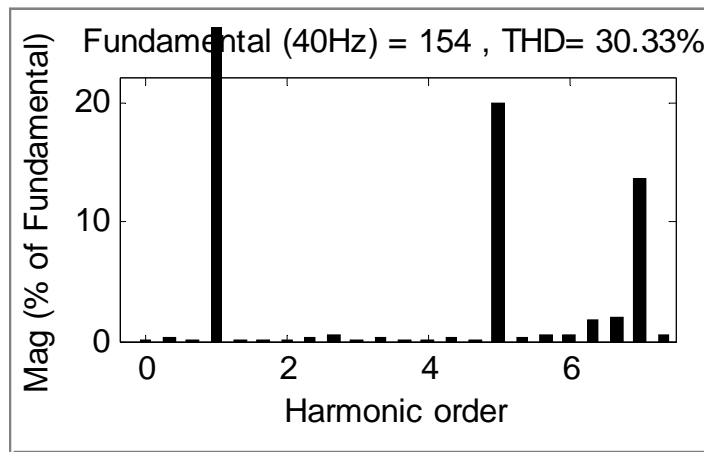


Figure 15: Harmonic Spectrum of output voltage in Carrier based method for 40Hz.

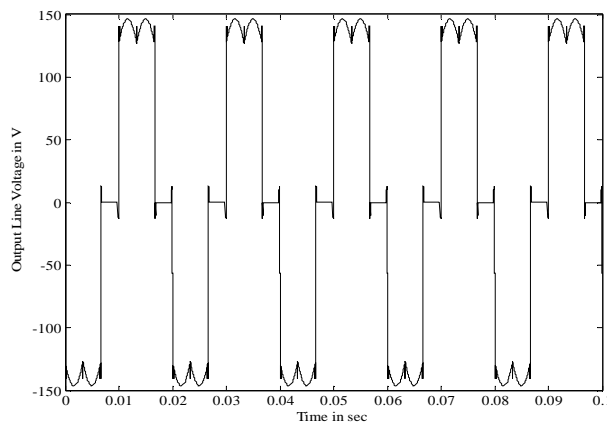


Figure 16: Output voltage in carrier method for 50Hz.

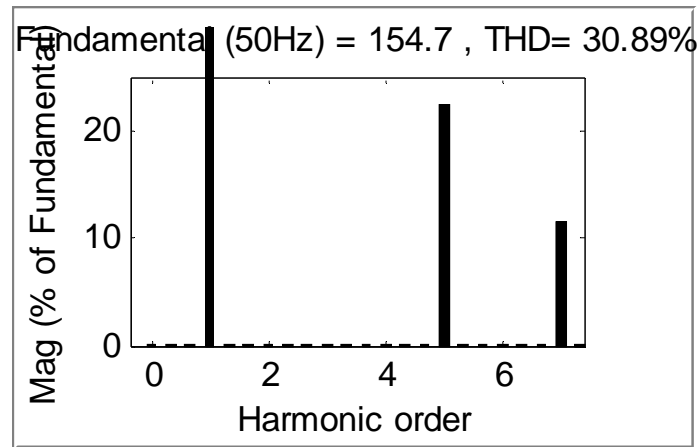


Figure 17: Harmonic Spectrum of output voltage in Carrier based method for 50Hz.

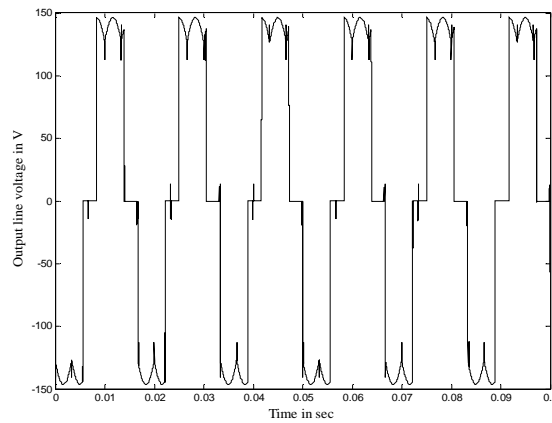


Figure 18: Output voltage in carrier method for 60Hz.

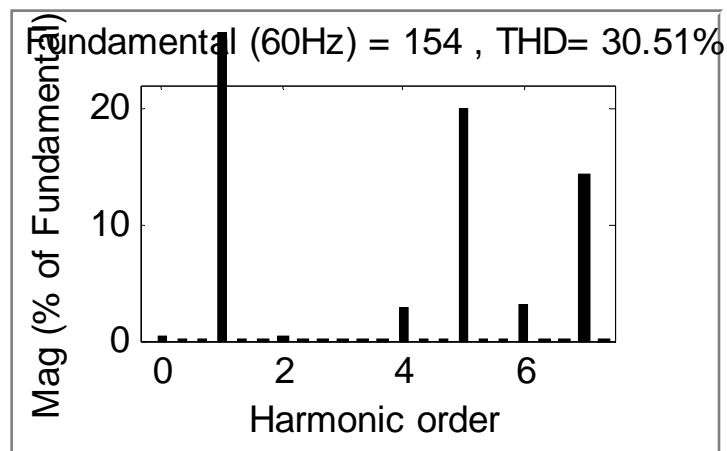


Figure 19: Harmonic Spectrum of output voltage in Carrier based method for 60Hz.

The output voltage waveform in Venturini modulation Method at 40Hz frequency is given in the fig.1 and its corresponding Harmonic Spectrum is shown in the fig.15. The output voltage and its corresponding Harmonic Spectrum at a frequency of 50Hz from SVM Method are given in the fig.16 and fig.17 respectively. Similarly the output voltage and its Harmonic Spectrum waveform at 60Hz using Carrier based method are given in the fig.18 and fig.19. The values of third, fifth and seventh harmonics measured in terms of fundamental output voltage at various frequencies using different modulation techniques are being tabulated in the Table.1.

Table 1: Harmonics in terms of percentage of fundamental output voltage.

Frequency Of output voltage	Third Harmonic content (%)			Fifth Harmonic content (%)			Seventh Harmonic content (%)		
	Venturini	SVM	Carrier	Venturini	SVM	Carrier	Venturini	SVM	Carrier
40 Hz	0.9	0.08	0.9	1.8	0.18	20	1.25	0.11	13
50 Hz	2.3	0.06	0.2	0.8	0.13	23	2.3	0.24	12
60 Hz	1.4	0.08	0.07	0.3	0.12	20	1.8	0.07	14

Table 2: Voltage Transfer Ratios of different modulation methods.

Modulation Method	Input Voltage in V	Output Voltage in V	Voltage Transfer Ratio
Venturini	540	467	86 %
SVM	460	400	86 %
Carrier	230	155	67 %

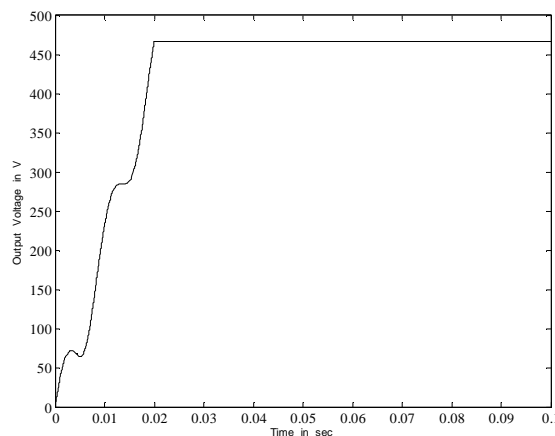


Figure 20: Fourier analysis of output voltage for $V_{in} = 540$ V in Venturini method for 50Hz.

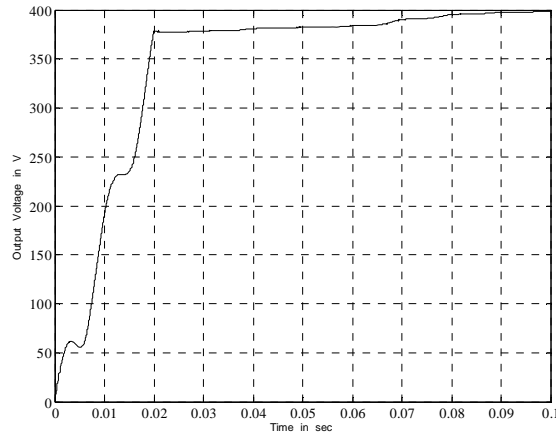


Figure 21: Fourier analysis of output voltage for $V_{in} = 460$ V in SVM method for 50Hz.

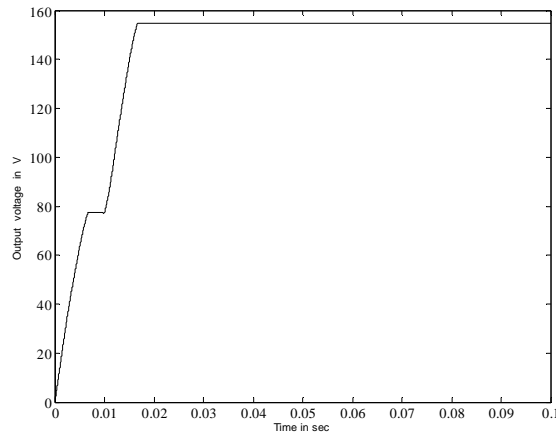


Figure 22: Fourier analysis of output voltage for $V_{in} = 230$ V in Carrier based method for 50Hz.

Fig.(20 – 22) shows the Fourier analysis of output voltages for three modulation methods with an output frequency of 50Hz. The input and output voltages and voltage transfer ratio are given in table.2. The result shows that venturini and SVM methods gives 86% of voltage transfer ratio whereas carrier based method is very poor in terms of voltage transfer ratio.

Fig.(23-24) shows the speed torque response of three phase induction motor using venturini switching algorithm. The dynamic performance of the motor is analyzed. At $t=0$ sec motor is started with no load condition. Steady state is reached at $t= 0.2$ sec. A load torque of 5 N-m is applied at $t=0.6$ sec. The steady state is reached at $t=0.65$ sec. The transient time taken is 0.05 sec.

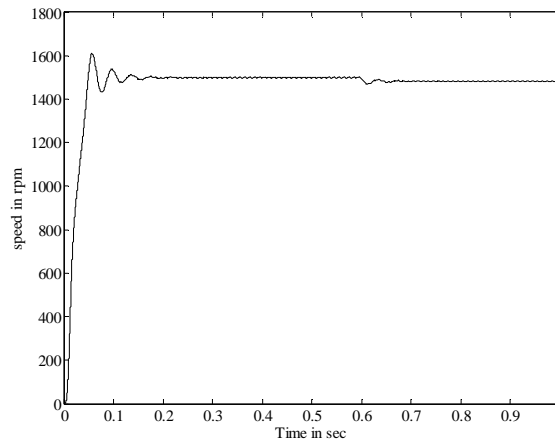


Figure 23: Speed response in venturini switching algorithm.

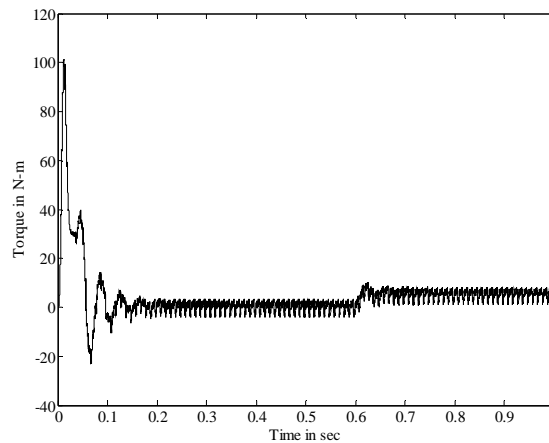


Figure 24: Torque response in venturini switching algorithm.

Fig.(25-26) shows the speed torque response of three phase induction motor using SVM algorithm. The dynamic performance of the motor is analyzed. At $t=0$ sec motor is started with no load condition. Steady state is reached at $t= 0.2$ sec. A load torque of 5 N-m is applied at $t=0.6$ sec. The steady state is reached at $t=0.7$ sec. The transient time taken is 0.1 sec.

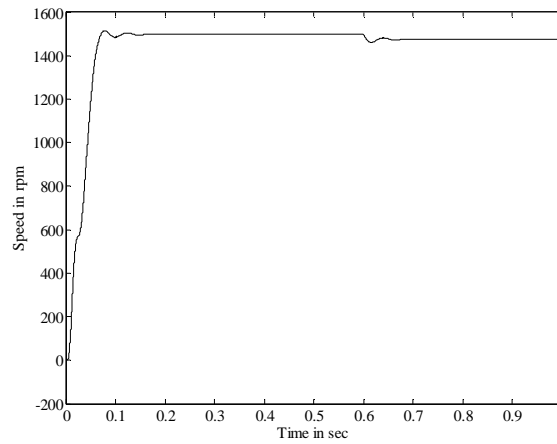


Figure 25: Speed response in SVM algorithm.

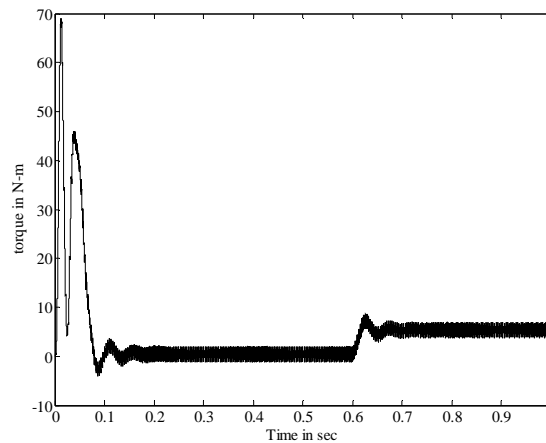


Figure 26: Torque response in SVM algorithm.

Fig. (25-26) shows the speed torque response of three phase induction motor using carrier based switching algorithm. The dynamic performance of the motor is analyzed. At $t=0$ sec motor is started with no load condition. Steady state is reached at $t=0.5$ sec. A load torque of 5 N-m is applied at $t=0.6$ sec. The steady state is reached at $t=0.95$ sec. The transient time taken is 0.35 sec.

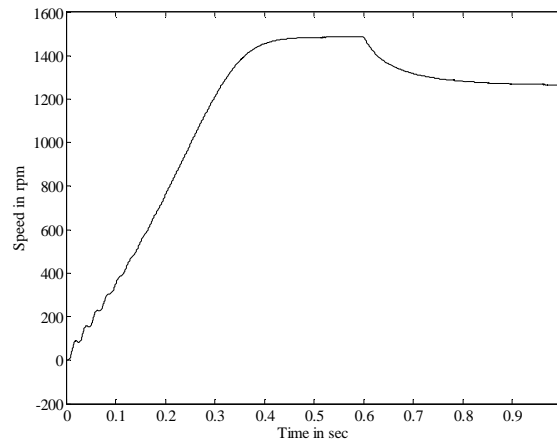


Figure 27: Speed response in venturini modulation method.

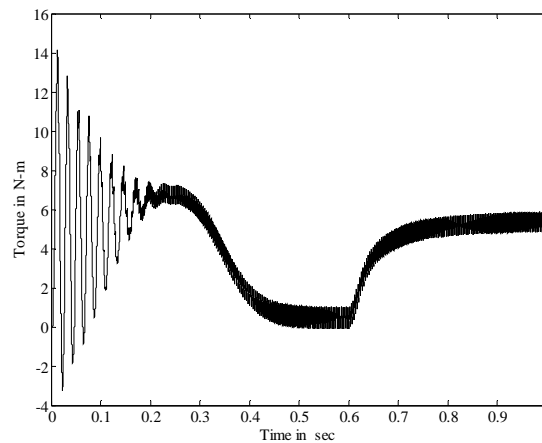


Figure 28: Torque response in venturini modulation method.

Conclusion

Three different switching algorithms of Matrix converter namely, Venturini switching algorithm, Space Vector Modulation and Carrier based switching algorithms are simulated and analyzed for matrix converter fed induction motor drive. Implementation of Space Vector Modulation technique involves sector identification and intricate calculations. The implementation of Venturini method and Carrier based modulation techniques does not require sector identification and intricate calculations. But Venturini method involves injection of harmonics to improve the voltage transfer ratio. The simulation results are analyzed for harmonics present in the output voltage. Lower order odd harmonic contents of the output voltage for different frequencies of operation is very less in terms of their fundamental component of output voltage with Space Vector Modulation technique as compared to other methods. In terms of output

voltage transfer ratio, both Space Vector modulation and Venturini methods give the maximum of 86.6%. The speed torque response of the motor is absorbed with all the switching algorithms. The dynamic performance of the motor is better with Venturini and SVM techniques in terms of response time and torque ripple is less with SVM technique.

References

- [1] Alesina, A and M. G. B. Venturini, "Analysis and design of optimum amplitude nine-switch direct AC-AC converters," *IEEE Trans. Power Electron.*, vol. 4, pp. 101-112, Jan. 1989.
- [2] Apap, M, Clare, J.C, Wheeler P.W and Bradley.K.J. "Analysis and Comparison of AC-AC Matrix Converter Control Strategies", *PESC03, IEEE 34th Annual conference on Power Electronics*, Vol. 3, pp. 1287-1292, June 2003.
- [3] AzeddineBendiabdellah, GhalemBachir "A Comparative Performance Study Between A Matrix Converter and a Three-Level Inverter Fed Induction Motor" *ActaElectrotechnica Et Informatica* No. 2, Vol. 6, 2006
- [4] Dehnavi, S.M.D.; Mohamadian, M.; Yazdian, A.; Ashrafzadeh, F.; "Space Vectors Modulation for Nine-Switch Converters" *Power Electronics, IEEE Transactions on* June 2010 Volume: 25 On page(s): 1488 - 1496
- [5] GhalemBachir, AzeddineBendiabdellah "A comparative study between two control strategies for matrix converter" *Advances in Electrical and Computer Engineering*, Volume 9, Number 2, 2009.
- [6] Helle.L, K. B. Larsen, A. H. Jorgensen, S. Munk-Nielsen, and F. Blaabjerg, "Evaluation of modulation schemes for three-phase to three phase matrix converters," *IEEE Trans. Ind. Electron.*, vol. 51, no. 1, pp. 158-171, Feb. 2004.
- [7] Huber.L and D. Borojevic, "Space vector modulation with unity input power factor for forced commutated cycloconverters," in *Conf. Rec.IEEE-IAS Annu. Meeting*, 1991, pp. 1032-1041.
- [8] Wheeler.P.W, J. Rodriguez, J. C. Clare, L. Empringham, and A. Weinstein, "Matrix converter: A technology review," *IEEE Trans. Ind. Electron.*, vol. 49, no. 2, pp. 276-288, Apr. 2002.
- [9] Yoon and S. K. Sul, "Carrier-based modulation technique for matrix converter," *IEEE Trans. Power Electron.*, vol. 21, no. 6, pp. 1691-1703, Nov. 2006.
- [10] Zhang.L, C.Watthanasarm, W.Shepherd "Analysis and comparison of control techniques for ac - ac converter" *IEE Proc-Electr. Power Appl.* Vol 145, 1998
- [11] Zhou and D. Wang, "Relationship between Space-Vector Modulation and Three-Phase Carrier-Based PWM: A Comprehensive Analysis," *IEEE Transactions on Industrial Electronics*, Vol. 49, Issue 1, pp. 186-196, Feb. 2002.